Simulation of electron trajectory for E-type electron gun in the magnetic focusing & deflection system

TAO NING[a,b,*], ZHIMIN LI[a], MAOLIN ZHANG[a]
[a] *School of Advanced Materials and Nanotechnology, Xidian University, No. 2, South TaiBai Road, Xi'an, 710071, China*
[b] *Construction Engineering Research Institute of the Department of Logistics, PLA, No.16, North Jinghua Road, Xi'an, 710032, China*

The e-type electron gun is widely used in electron beam evaporation due to its good evaporation ability. However, it also suffers from the drawbacks of poor focusing and electron beam divergence. In this paper, a deflection system consisting of permanent magnets is established, and the magnetic field is numerically simulated using the boundary element method. Further, electron trajectory in the magnetic field is calculated using the Runge-Kutta method, supplemented by a discussion on the relationship between the focusing ratio and the magnetic charge density, magnetic pole pitch, initial electron velocity and incident angle.

(Received May 08, 2018; accepted February 12, 2019)

Keywords: E-type electron gun, Deflection system, Numerical simulation, Electron trajectory

1. Introduction

Electron beam evaporation is a coating technique in which the coating material is evaporated by the heat generated by accelerated electrons hitting on it, and then deposited on the surface of the workpiece to form a film [1-3]. Since films formed by means of electron beam evaporation are characterized by strong adherence and fine surface grains, this technique has found uses in a wide range of applications [4-5]. The electron gun is an essential component in electron beam evaporation coating machines. Depending on the type of electron evaporation source used, electron guns can be divided into annular guns, straight guns, hollow-cathode guns and e-type guns.

Due to its good evaporation ability, the e-type gun has been widely used in various applications. E-type electron gun evaporation produces films of high quality with excellent uniformity, allows for multi-layer evaporation, and ensures high film purity [6-7]. The electron beam emitted by the e-type electron gun generates a gyro deflection under the influence of a permanent magnet, with a deflection angle up to 270°. Using a scanning mechanism, the electron beam can be made to pass through an electromagnetic coil and to hit the surface of the target material in the crucible [8]. By adjusting the intensity of the magnetic field, the beam spot can be manipulated to hit anywhere on the surface of the target material in the crucible. However, in this system, after passing through the deflection field the deflected electron beam is likely to lose its focus, and has less sputtering power, resulting in uneven thickness across the deposited film. This may seriously degrade the quality of the film [9].

In order to study the focusing and deflection characteristics of e-type electron guns, the most important thing is to obtain the magnetic field distribution within the electron gun, and then work out the trajectory of the electrons by analyzing their movement in the magnetic field [10-13]. In this work, a deflection system consisting of permanent magnets is established to simulate the direction of the magnetic force line at each point. Then, the Runge-Kutta method [14-15] is used to simulate the electron trajectory in the magnetic field.

2. Experiments

The e-type electron gun exhibits better focusing characteristic than other types. The magnetic field deflection system designed in this work is illustrated in Fig. 1. The sizes of L_1, H_1, L_2 and H_2 are 0.05, 0.005, 0.008 and 0.008 m, respectively. The soft iron pieces at each side of the magnetic field deflection system are connected to a permanent magnet in between. As the magnetic permeability of soft iron can be as high as 20000 H/m, the object under consideration is uniformly magnetized. The lines of magnetic force emerge from the surfaces of A and B and terminate at the surfaces of A' and B'. The magnetic pole surfaces are parallel to each other, so the magnetic charge density of each magnetic pole surface is constant.

The equivalent surface magnetic flux is used to work out the magnetic field intensity distribution [16-17], and the calculation process and program are presented in Appendix 1. Furthermore, the magnetic induction intensity

at any point in the magnetic field can be obtained through transformation. The process and program for calculating the magnetic induction intensity is shown in Appendix 2.

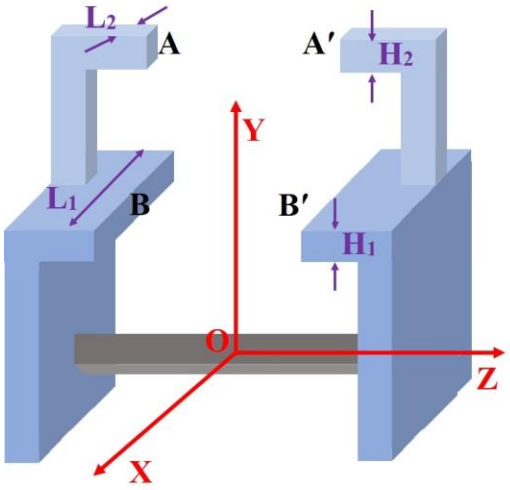

Fig. 1. Schematic diagrams of the magnetic pole for magnetic deflection system

3. Results

3.1. Simulation results of the deflection-focusing magnetic field

Fig. 2 shows the distribution of magnetic field lines on the plane X =0 m. It can be found that the lines of magnetic force experience greater deflection at positions close to the magnetic poles on both sides, and the lines of magnetic force all run along the Z direction on the symmetry plane in the middle. Meanwhile, it can be found that the directions of the magnetic fields at the points X = -0.01 m and X = 0.01 m are identical, respectively. It can be concluded that the movement trajectory of the electrons at one side of the symmetry plane is symmetrical to that of electrons at the other side. Therefore, it is only necessary to analyze the movement trajectory of electrons on half of the plane.

On the other hand, as the lines of magnetic force on the symmetry plane only have a Z-direction component, electrons emitted on the symmetric plane would not deviate from the symmetry plane, making it easier to control focusing. Moreover, the magnitude of the magnetic field intensity is mainly determined by the first (magnetic pole A) and second magnetic poles (magnetic pole B) while the third magnetic pole contributes less to the magnetic field intensity due to its small size and farther distance from the electron deflection region. Therefore, the deflection of electrons is mainly affected by the first and second magnetic poles.

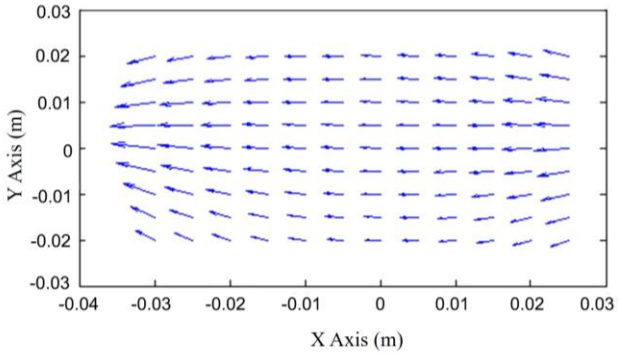

Fig. 2. Distribution of magnetic field lines on X =0 m plane

3.2. Trajectory of electrons in deflection focusing system

In electronic optics studies, the Runge-Kutta method [14-15] is commonly used to solve the electron motion equations. Since the electrons under consideration are only affected by the force of the magnetic field, we can consider only the effect of the Lorentz force on the trajectory of the electrons in the magnetic field. The Lorentz force is known as following

$$F=-eVB \quad (1)$$

where, F is the Lorentz force acting on the electrons, e is the charge of the electrons, V is the electron velocity, and B is the magnetic field strength. The Runge-Kutta method with fourth-order of the differential equation was used to solve the above equations. The program for describing the electron trajectory is shown in Appendix 3.

The trajectory of electron focusing can be divided into two parts, one is the trajectory focusing of electrons whose initial emission are on the asymmetric plane, and the others are on the symmetry plane.

A force analysis of the electron moving in the magnetic field shows that the electron always sustains a force pointing towards the symmetry plane during movement. Therefore, electrons emitted from the Z axis exhibit good focused characteristics. Assuming two electrons are emitted from two symmetrical positions on either side of the Z axis, the projection of the two electron trajectories on the XY plane is as shown in Fig. 3, where it can be seen that the two electrons intersect on the symmetry plane. Fig. 4 is a 3D diagram depicting the movement of electrons emitted at one side, revealing the trajectory pattern.

The exit positions of the electrons in Fig. 3 are Z = -0.025 m and Z = 0.025 m, respectively. Thus, the trajectories of electrons emitted from the center should occur between these two trajectories. Therefore, the chosen case is the one with the greatest deflection. It is totally feasible to use such an extreme case as a typical

example to analyze the trajectories of this class of electrons.

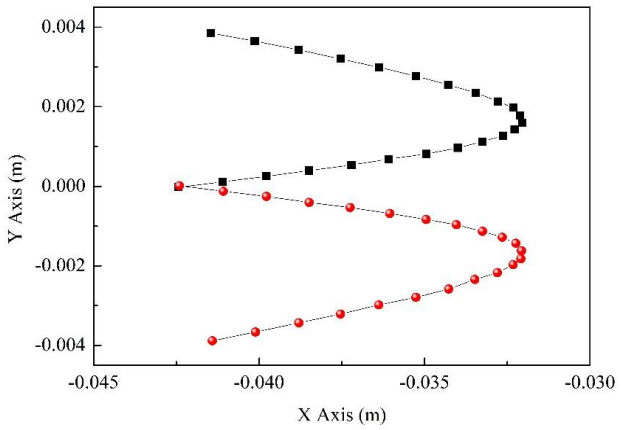

Fig. 3. Trajectory of electrons emitted from both sides of symmetry axis

In Fig. 4, it can be found that at the beginning of the electron movement, the electron first spirals in the positive direction of Z, and then deflects in the opposite direction. On the other hand, the deflection radius becomes lager as the movement of electrons, indicating that the electron is in a region with high magnetic field strength during its initial stage of movement. It can be seen from Fig. 3 that at position Y = -0.02 m, the electron has good focus characteristic.

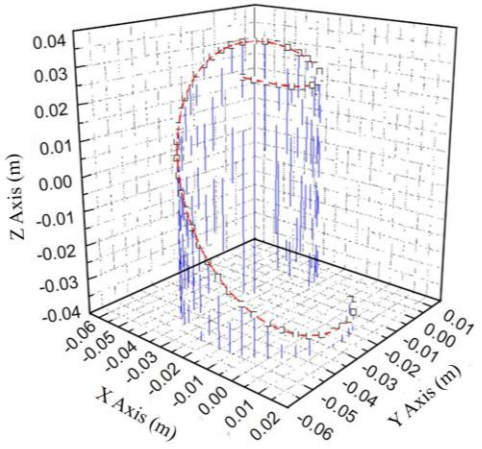

Fig. 4. The 3D trajectory of electron emitted from one side of symmetry axis

In the former case, as the movement of electrons in the magnetic field is three-dimensional, the pattern of their trajectories is difficult to establish. However, if the electron is emitted from the symmetry plane, the symmetrical characteristic of the magnetic poles in relation to the symmetry plane dictates that the magnetic force lines on the symmetry plane are perpendicular to it. So, if the electron is emitted from the symmetry plane and the velocity of the electron has no component in the Z direction, it can be ensured that the electron will move on the symmetry plane.

Since there are multiple factors that affect the trajectory of electrons, the parameters, including magnetic charge density (Q), distance between the first and the second magnetic poles (H_{AB}), initial velocity (V) of the electron and the electron exit angle are discussed in turn. The focusing ratio (d_2/d_1) is defined as the ratio of the width of the electron beam spot at endpoint d_2 to the width of the original electron beam d_1. The focusing result can be studied by characterizing the relationship between the focusing ratio and various parameters.

Fig. 5 shows the effect of the magnetic charge density (Q) on the focusing of electrons (d_2/d_1). It shows clearly that electron focusing is optimal when the magnetic charge density is 0.055 Wb/m^2. Deviating from this value, either higher or lower, could result in poor focus or no focus at all. The relationship between H_{AB} (the distance between the first and second pole) and the electron focusing ratio (d_2/d_1) is also showed in Fig. 5. It can be observed that H_1 has no significant effect on the focusing of electrons. However, the experiment results demonstrated that when the height of the electron's trajectory exceeds 1/2 H_{AB} of the first pole, its trajectory is no longer focused. The analysis of the magnetic field strength reveals that the intensity of the magnetic field rapidly decreases beyond 1/2 H_{AB} of the first pole, and the electron rotation radius increases rapidly, which means that the electrons are no longer focused. This means that the distance between the first and second pole needs to be adjusted according to the electron velocity.

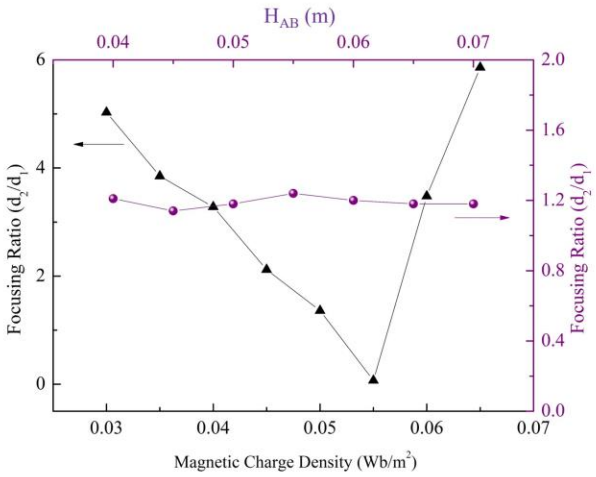

Fig. 5. Relationship between magnetic charge density, H_{AB} and electron focusing ratio (d_2/d_1)

Fig. 6 shows the relationship between the electron initial velocity, exit angle and the electron focusing ratio. Based on the equation for solving the rotating radius of the electron in the magnetic field, we can find that the velocity and the radius are directly proportional to each other. The best focusing can be achieved when the initial velocity is 2

◊ 10^7 m/s. A lower initial velocity would render the electron out of focus, while a higher initial velocity would cause a rapid increase of the focusing ratio.

The relationship between the electron exit angle and the electron focusing ratio is also shown in Fig. 6, where the exit angle is the angle between the electron exit velocity and the X axis. It is obvious that the best focusing can be achieved when the electron is emitted along the X coordinate. Therefore, it is necessary to ensure that the electron is emitted straight in the direction along the X axis so as to obtain the best focusing effect.

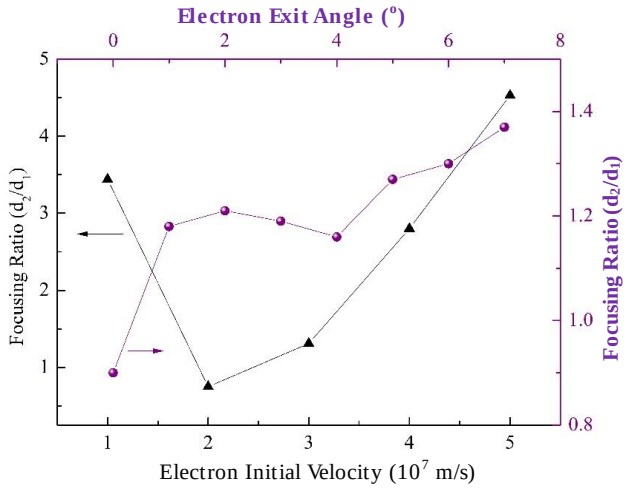

Fig. 6. Relationship between electron initial velocity, exit angle and electron focusing ratio

4. Conclusions

In this work, a deflection system consisting of permanent magnets was established in order to study the focus deflection characteristic of the e-type electron gun. The boundary element method was used to simulate the magnetic field in the open region. Runge-Kutta method was used to simulate and calculate the trajectory of the electrons in the magnetic field. The relationship between the focusing ratio and magnetic charge density, magnetic pole pitch, initial electron velocity and incident angle were explored.

Acknowledgements

This work was supported by the National Natural Science Foundation of China (grant numbers 61701369); Fundamental Research Funds for the Central Universities (grant numbers JB181407).

References

[1] Barranco Angel, Borras Ana, Gonzalez-Elipe Agustin, et al., Progress in Materials Science **76**, 59 (2016).
[2] Wu Qingying, Bing Wenzeng, Long Xinggui, et al., Vacuum **86**, 2162 (2012).
[3] N. I. Kato, Y. Kohno, H. Saka, Journal of Vacuum Science & Technology A **17**, 1201 (1999).
[4] Rill Michael, Plet Christine, Thiel Michael, et al., Nature Materials **7**, 543 (2008).
[5] Hak Ki Yu, Thin Solid Films **653**, 57 (2018).
[6] L. Yu Ovchinnikova, V. I. Shvedunov, Instruments and Experimental Techniques **58**, 399 (2015).
[7] Dikshit Biswaranjan, M. S. Bhatia, IEEE Transactions on Electron Devices **57**, 939 (2010).
[8] Munawar Iqbal, Ghalibul Islam, Safa Saleem, W. B. Herrmannsfeldt, Vacuum **101**, 157 (2014).
[9] Munawar Iqbal, G U. Islam, I. Misbah, O. Iqbal, Z. Zhou, Review of Scientific Instruments **85**, 66106 (2014).
[10] David John, Ives R. Lawrence, Tran Hien, et al., IEEE Transactions on Plasma Science **36**, 156 (2008).
[11] M. V. Vilkov, M. Yu. Glyavin, A. L. Goldenberg, et al., Technical Physics Letters **38**, 680 (2012).
[12] Y. F. Kang, J. Zhao, J. Y. Zhao, et al., Laser and Particle Beams **32**, 487 (2014).
[13] M. Iqbal, G U. Islam, Z. Zhou, Y. Chi, Review of Scientific Instruments **84**, 116107 (2013).
[14] H. B. Sun, Y. J. Pei, A. G Xie, High Energy Physics and Nuclear Physics-Chinese Edition **29**, 95 (2005).
[15] Tian Jin-Shou, Zhao Bao-Sheng, Wu Jian-Jun, et al., Acta Physica Sinica **55**, 3368 (2006).
[16] Liping Wang, John Rouse, Eric Munro, Haoning Liu, Xieqing Zhu, Optik **119**, 90 (2008).
[17] S. Hirohata, T. Kosugi, H. Sawaragi, R. Aihara, K. Gamo, Journal of Vacuum Science & Technology B **10**, 2814 (1992).

*Corresponding author: 181706548@qq.com

Supporting Information

Appendix 1---- used to work out the magnetic field intensity distribution

```
#include<cmath>
#include<iostream>
using namespace std;
double bisimp(double a,double b, double z,double eps, double J1, .
double Jh, double X, double Y, double Z, double Q1);
double simp(double x,double z, double eps, double J1, double Jh,
double X, double Y, double Z, double Q1);
void bisimpfs(double y[], double J1, double Jh);
double bisimpf(double x,double y, double z, double X,
double Y, double Z, double Q1);
double abcd(double X,double Y, double Z, double L1,
double H1, double H2, double L2,
double Q1, double Q2,double Q3);
double abcd(double X,double Y, double Z, double L1,
            double H1, double H2, double L2,
double Q1, double Q2,double Q3)
{for(I1=-0.5*L1;I1<=0.5*L1;I1=I1+0.002)
{for(J1=0.0;J1<=high1;J1=J1+0.0005)
    { result1=bisimp(I1,I1+0.001,0.5*width,10e-10,J1,0.001,X,Y,Z,Q1)+result1;
    result3=bisimp(I1,I1+0.001,-0.5*width,10e-10,J1,0.001,X,Y,Z,Q1*(-1))+result3;
        }
    }
    for(I2=-0.5*L2;I2<=0.5*L2;I2=I2+0.001)
    {   for(J2=H1;J2<H1+H2;J2=J2+0.001)
        {   result2=bisimp(I2,I2+0.001,0.5*width,10e-10,J2,0.001,X,Y,Z,Q2)+result2;
    result4=bisimp(I2,I2+0.001,-0.5*width,10e-10,J2,0.001,X,Y,Z,Q2*(-1))+result4;
        }
    }
    for(I3=L2-0.5*L3;I3<=L2+0.5*L3;I3=I3+0.0001)
    result=result2+result4+result3+result1+result6+result5;
    return result;
}
double bisimp(double a,double b, double z,double eps, double J1,
  double Jh, double X, double Y, double Z, double Q1)
{   int n,j;
    double h,d,s1,s2,t1,x,t2,g,s,s0,ep;
    n=1; h=0.5*(b-a);
    d=fabs((b-a)*1.0e-06);
    t1=h*(s1+s2);
    s0=1.0e+35;  ep=1.0+eps;
```

```
    while (((ep>=eps)&&(fabs(h)>d))||(n<16))
        s=(4.0*t2-t1)/3.0;ep=fabs(s-s0)/(1.0+fabs(s));
        n=n+n; s0=s; t1=t2; h=h*0.5;
    }
    return(s);
}
double simp(double x,double z, double eps, double J1,
            double Jh, double X, double Y, double Z, double Q1)
{   int n,i;
    double y[2],h,d,t1,yy,t2,g,ep,g0;n=1;
    bisimpfs(y, J1, Jh);
    h=0.5*(y[1]-y[0]);d=fabs(h*2.0e-06);t1=h*(bisimpf(x,y[0],z, X,Y,Z,Q1)+bisimpf(x,y[1],z, X,Y,Z,Q1));
    ep=1.0+eps; g0=1.0e+35;
    while (((ep>=eps)&&(fabs(h)>d))||(n<16))
    { yy=y[0]-h;t2=0.5*t1;for (i=1;i<=n;i++)
        { yy=yy+2.0*h;
          t2=t2+h*bisimpf(x,yy,z,X,Y,Z,Q1);
        }
        g=(4.0*t2-t1)/3.0;
        ep=fabs(g-g0)/(1.0+fabs(g));
        n=n+n; g0=g; t1=t2; h=0.5*h;
    }
    return(g);
}
void bisimpfs(double y[], double J1, double Jh)
{   y[0]=J1;   y[1]=J1+Jh;     return;
}
double bisimpf(double x,double y, double z, double X, double Y, double Z, double Q1)
{   double r;
    r=Q1*(1/sqrt(pow((x-X),2)+pow((y-Y),2)+pow((z-Z),2)));      return(r);
}
```

Appendix 2----used to calculate the magnetic induction intensity

```
#include <iostream>
#include"abc.cpp"
#include<fstream>
#include<cmath>
using namespace std;
int main()
{ double BX0,BY0,BZ0;
double x0,y0,z0;
long double k0(0.00001),k1(100000);
double width(0.1),L1(0.05),H1(0.005),          H2(0.008),L2(0.008),  Q1(0.05),Q2(0.05),Q3(0.05);
double L(0.005),B;
```

```
cout<<"please input X ";
cin>>x0;
ofstream outB("outB.txt");
for(y0=high_2;y0<=high_1;y0=y0+0.01)
{for(z0=-0.3*width;z0<=0.3*width;z0=z0+0.01)
{BX0=-(abcd(x0+k0,y0,z0,width,L1,H1,H2,L2,Q1,Q2,Q3)
-abcd(x0,y0,z0,width,L1,H1,H2,L2,Q1,Q2,Q3))*k1;
BY0=-(abcd(x0,y0+k0,z0,width,L1,H1,H2,L2,  L3,H3,  Q1,Q2,Q3)
      -abcd(x0,y0,z0,width,L1,H1,L2,H2,L3,H3,Q1,Q2,Q3))*k1;
BZ0=-(abcd(x0,y0,z0+k0,width,L1,H1,H2,L2,H3,L3,  Q1,Q2,Q3)
      -abcd(x0,y0,z0,width,  L1,H1,H2,L2,H3,L3,Q1,Q2,Q3))*k1;
B=sqrt(BY0*BY0+BZ0*BZ0);
cout<<"x="<<x0<<"  y="<<y0<<"  z="<<z0<<"  ";
cout<<"BX="<<BX0<<"  BY="<<BY0<<"  BZ="<<BZ0<<endl;
}
      }
      system("PAUSE");
      return 0;
}
```

Appendix 3----used to describe the electron trajectory

```
#include<iostream>
#include<stdio.h>
#include<cmath>
#include"abc.cpp"
#include<fstream>
#include<string>
using namespace std;
int main()
{ double x0(0.04),x1,y0(-0.02),y1,z0(0),z1;
  double l0(-3e7),l1,m0(0),m1,n0(0),n1;
  double p1,p2,p3,p4,q1,q2,q3,q4,r1,r2,r3,r4;
  double BX0,BX1,BY0,BY1,BZ0,BZ1,B1,B2;
  long double k(0.0000001),k1(10000000),g(17563),h(2.0e-10);
  double L(0),M,N(3.14159265359);
  int X(10);
  string str;
  cout<<"please input the name of your data";
  cin>>str;
cout<<"x     y     z\n";
cin>>x0>>y0>>z0;
cout<<"L\n";
cin>>L;
```

```
l0=l0*sin(L*N/180);
n0=n0*cos(L*N/180);
cout<<"BX    BY    BZ\n";
cin>>BX0>>BY0>>BZ0;
cout<<"H    N\n";
cin>>h>>N;
ofstream outF("1.txt");
BX0=-(abcd(x0,y0,z0)-abcd(x0-k,y0,z0))*k1;
BY0=-(abcd(x0,y0,z0)-abcd(x0,y0-k,z0))*k1;
BZ0=-(abcd(x0,y0,z0)-abcd(x0,y0,z0-k))*k1;
  M=-0.02;
    while(y0>=M)
    // for(int n=0;n<X;n++)
    {
      p1=((-g)*h*k1)*(m0*BZ0-n0*BY0);
      q1=((-g)*h*k1)*(n0*BX0-l0*BZ0);
      r1=((-g)*h*k1)*(l0*BY0-m0*BX0);       p2=((-g)*h*k1)*((m0+0.5*q1)*BZ0-(n0+0.5*r1)*BY0);
q2=((-g)*h*k1)*((n0+0.5*r1)*BX0-(l0+0.5*p1)*BZ0);       r2=((-g)*h*k1)*((l0+0.5*p1)*BY0-(m0+0.5*q1)*BX0);
p3=((-g)*h*k1)*((m0+0.5*q2)*BZ0-(n0+0.5*r2)*BY0);       q3=((-g)*h*k1)*((n0+0.5*r2)*BX0-(l0+0.5*p2)*BZ0);
r3=((-g)*h*k1)*((l0+0.5*p2)*BY0-(m0+0.5*q2)*BX0);
      p4=((-g)*h*k1)*((m0+q3)*BZ0-(n0+r3)*BY0);
      q4=((-g)*h*k1)*((n0+r3)*BX0-(l0+p3)*BZ0);
      r4=((-g)*h*k1)*((l0+p3)*BY0-(m0+q3)*BX0);
      l1=l0+1/6.0*(p1+2*p2+2*p3+p4);
      m1=m0+1/6.0*(q1+2*q2+2*q3+q4);
      n1=n0+1/6.0*(r1+2*r2+2*r3+r4);       x1=x0+1/6.0*(h*l0+h*(l0+0.5*p1)+h*(l0+0.5*p2)+h*(l0+p3));
y1=y0+1/6.0*(h*m0+h*(m0+0.5*q1)+h*(m0+0.5*q2)+h*(m0+q3));
z1=z0+1/6.0*(h*n0+h*(n0+0.5*r1)+h*(n0+0.5*r2)+h*(n0+r3));
      cout<<"x="<<x1<<"  y="<<y1<<"  z="<<z1<<endl;
      outF<<x1<<"  "<<y1<<"  "<<z1<<endl;
      BX1=-(abcd(x1,y1,z1)-abcd(x1-k,y1,z1))*k1;
      BY1=-(abcd(x1,y1,z1)-abcd(x1,y1-k,z1))*k1;
      BZ1=-(abcd(x1,y1,z1)-abcd(x1,y1,z1-k))*k1;
      x0=x1;y0=y1;  z0=z1;  l0=l1;  m0=m1;  n0=n1;
      BX0=BX1;  BY0=BY1;  BZ0=BZ1;
    }
  system("PAUSE");
  return
```